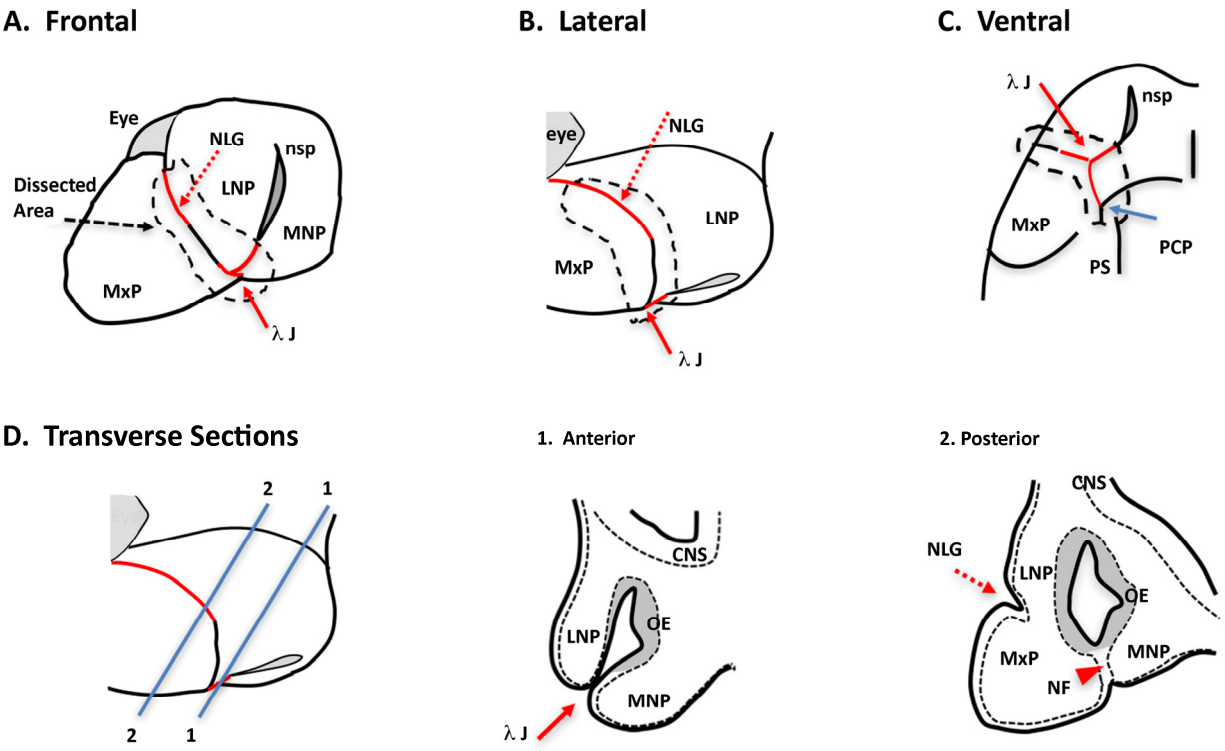

Figure S1. Schematic representation of E11.5 upper mouse face with landmarks pertinent to the scRNA-seq analysis.

Frontal **(A),** lateral **(B)** and ventral **(C)** cartoons of the left aspect of the upper mouse face. In (C) the lower jaw has been omitted to allow a view of the roof of the mouth. The regions marked with red lines are the fusion zones of the nasolacrimal groove (dashed red arrow) and the lambdoid junction (solid red arrow). The areas marked with the blacked dashed line approximate to the region of the face that was microdissected for scRNA-seq analysis seen in the three different views. (**D**) To the left is a lateral view of the face with the approximate location of the planes of section for the cartoon images of the transverse sections shown in 1. (middle panel, anterior) and 2. (right panel, posterior). CNS, central nervous system; λJ, lambdoid junction; LNP, lateral nasal prominence; MNP, medial nasal prominence; MxP, maxillary prominence; NF, nasal fin (red arrowhead indicating epithelial seam that exists after juxtaposition of prominences and before resolution to generate continuous mesenchyme); NLG, nasolacrimal groove; nsp, nasal placode; OE, olfactory epithelium (dark grey); PCP, primary choanal pit (blue arrow, the pit is not observed on a surface view, but lies under the angle of the tissue shown); PS, nascent palatal shelf (an outgrowth of the MxP). In the two transverse sections, the dashed lines represent the boundary between ectodermal and mesenchymal layers.

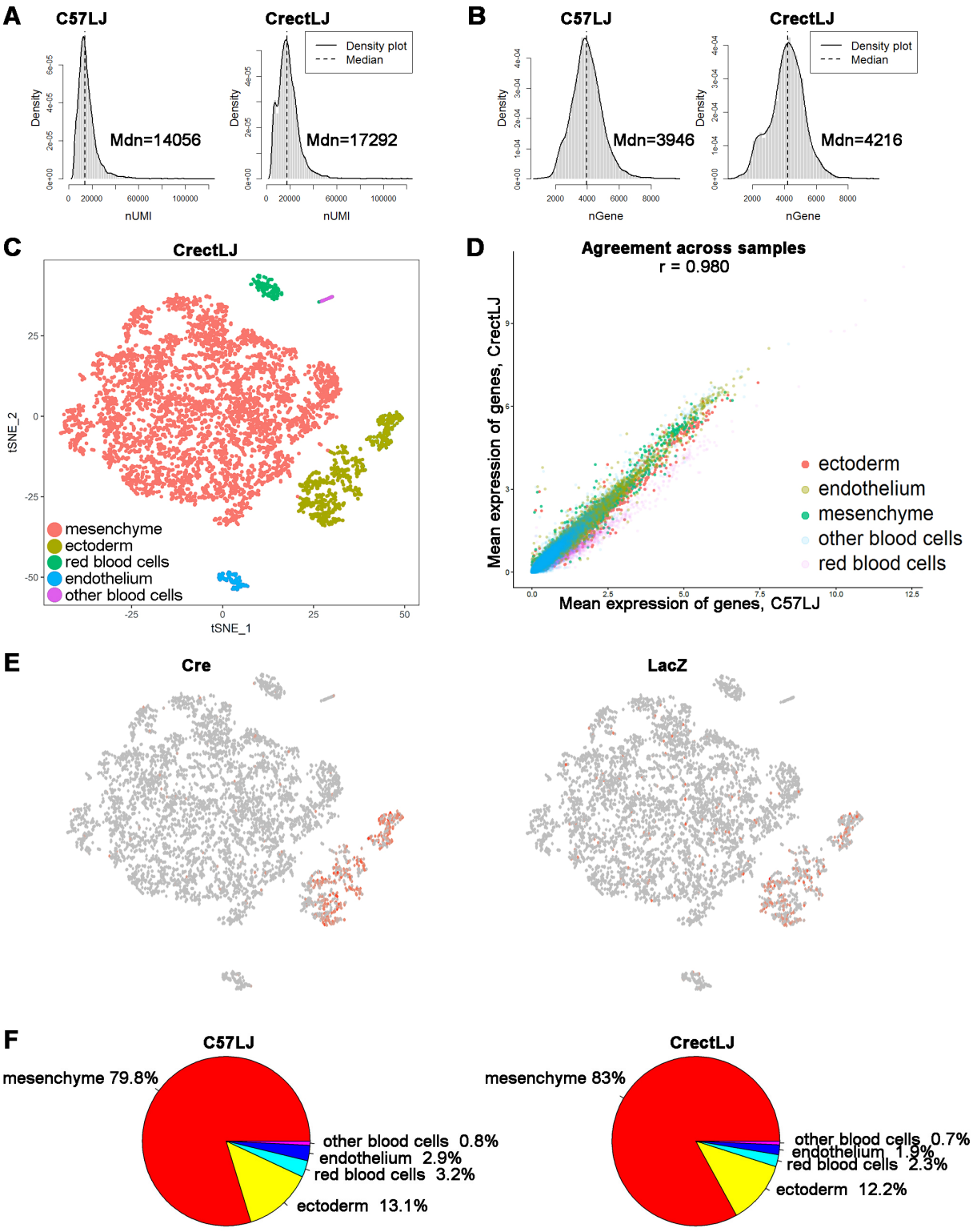

Figure S2. High reproducibility between the two scRNA-seq datasets from the lambdoidal junction.

(**A, B**) Distributions of the number of unique molecular identifiers (nUMI) (A) and the number of genes (nGene) (B) detected in two independent scRNA-seq datasets, C57LJ and CrectLJ. (**C**) tSNE plot of the CrectLJ dataset. In this dataset, 6673 cells were clustered (with 1417 variable genes, 10 Principal Components, and 0.6 resolution) with the Seurat package into the same 5 major clusters (mesenchyme, ectoderm, endothelial, red blood cells, and other blood cells) as the C57LJ dataset shown in Figure 1. (**D**) Agreement across samples shown by scatter plot of the average expression of each gene in each of the five cell types between C57LJ and CrectLJ. Pearson correlation (r) is 0.980 between the two experiments. The gene expression was computed by log2 ((UMI count for the gene/total UMI counts of the cell)*10000 +1). (**E**) Feature plots of *Cre* and *LacZ* genes in the CrectLJ dataset. In the feature plot, the normalized expression of the gene is superimposed on the tSNE plot with red-intensity indicating level of expression and grey indicating no expression. The expression of *Cre* and *LacZ* confirm the lineage of the ectodermal cells. (**F**) Pie charts show that the percentages by cell type in the C57LJ and CrectLJ datasets are similar. Mdn, median.

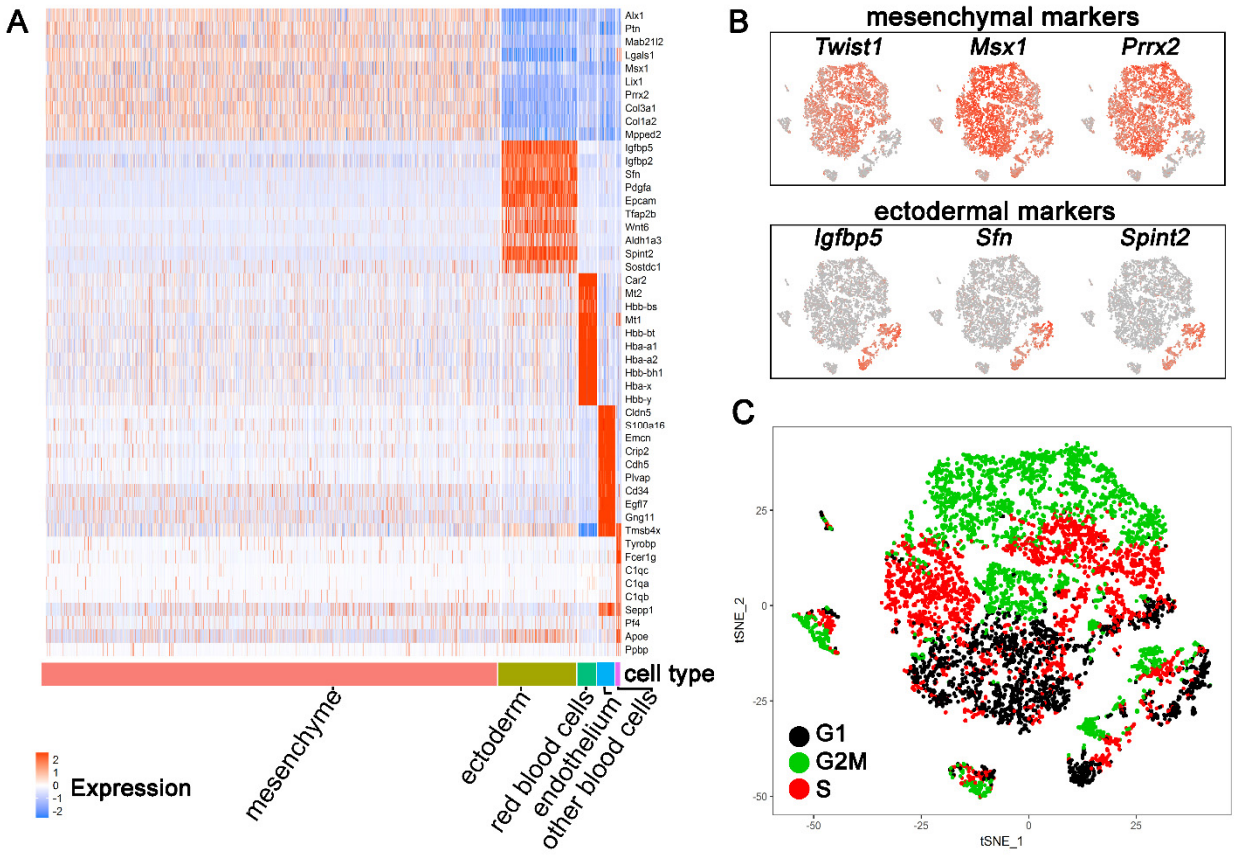

Figure S3. Major cluster gene markers and cell cycle effect on clustering.

(**A**) Heatmap for the top 10 most differentially expressed marker genes by avg_logFC of each cell type from the C57LJ dataset. Each row is the scaled expression of a gene. Each column is a cell. In the heatmap, red means higher expression, and blue means lower expression. The panel under the heatmap shows the annotation of the cell types. (**B**) Feature plots of ectodermal and mesenchymal markers genes in the C57LJ dataset. *Twist1*, *Msx1*, and *Prrx2* are mesenchymal markers. *Igfbp5*, *Sfn* and *Spint2* are markers for ectoderm. (**C**) The cell cycle phase was estimated using Seurat2 and superimposed on the tSNE plot of the C57LJ dataset. With the exception of the “other blood cell” cluster (small upper left cluster), cell cycle phase dominates the distribution of cells within each cell type. Note that we subsequently assessed if any mesenchyme (m0-m8) or ectoderm (e0-e11) cluster that was identified after cell cycle regression (Figs 2 and 5 respectively) showed any association with the state of the cell cycle. In general, we did not detect any major cell cycle differences between the various clusters identified that would indicate an effect of anatomical position and/or response to signaling.

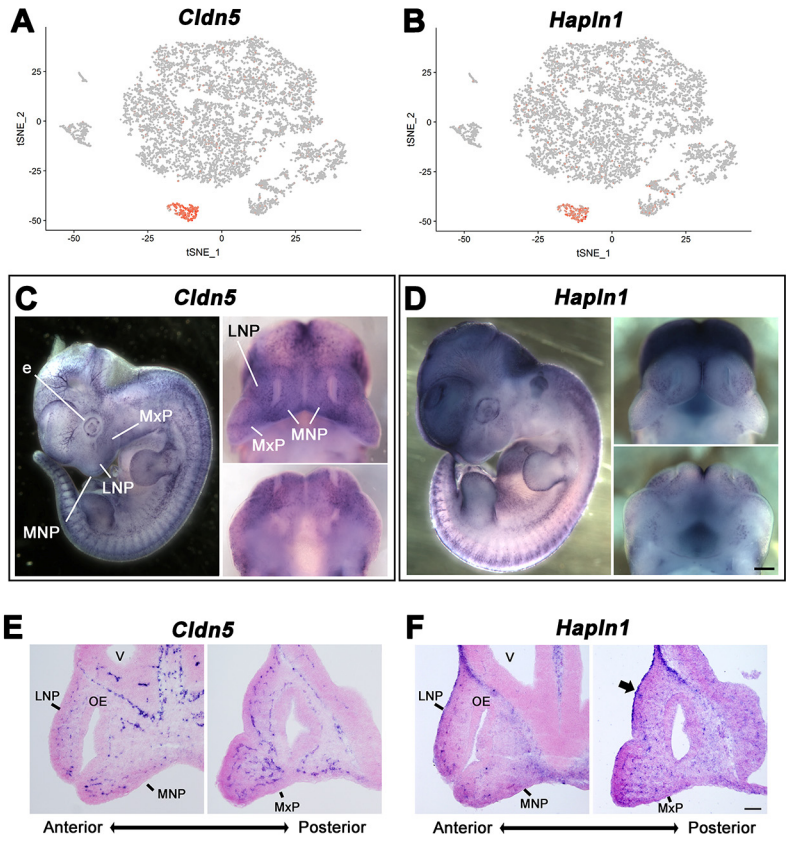

Figure S4. Visualization of markers for endothelial cells in the developing upper face.

(**A, B**) Feature plots of endothelium markers *Cldn5* and *Hapln1*. (**C, D**) Whole mount RNA *in situ* hybridization of E11.5 embryos with probes for either *Cldn5* or *Hapln1.* Three panels are shown for each probe. The left panel shows the lateral view of the whole embryo. The top right and bottom left panels show a frontal and palatal view of the head, respectively. In these latter two views the mandibular prominence has been removed for better visualization of the roof of the mouth. Scale bar, 500μM. (**E, F**) *In situ* hybridization on E11.5 frontal sections for *Cldn5* and *Hapln1.* The left section of each pair is more anterior and the right section more posterior as shown by the arrow beneath the panels. Scale bar, 100μM. Expression of both *Cldn5* and *Hapln1* occurs in the developing vascular system. *Hapln1* is also expressed in ectoderm as indicated by arrow in F, but most of these cells would not have been included in our microdissected samples. Sections are counterstained with nuclear fast red. e, eye; LNP, lateral nasal process; MNP, medial nasal process; MxP, maxillary prominence; oe, olfactory epithelium; V, ventricles.

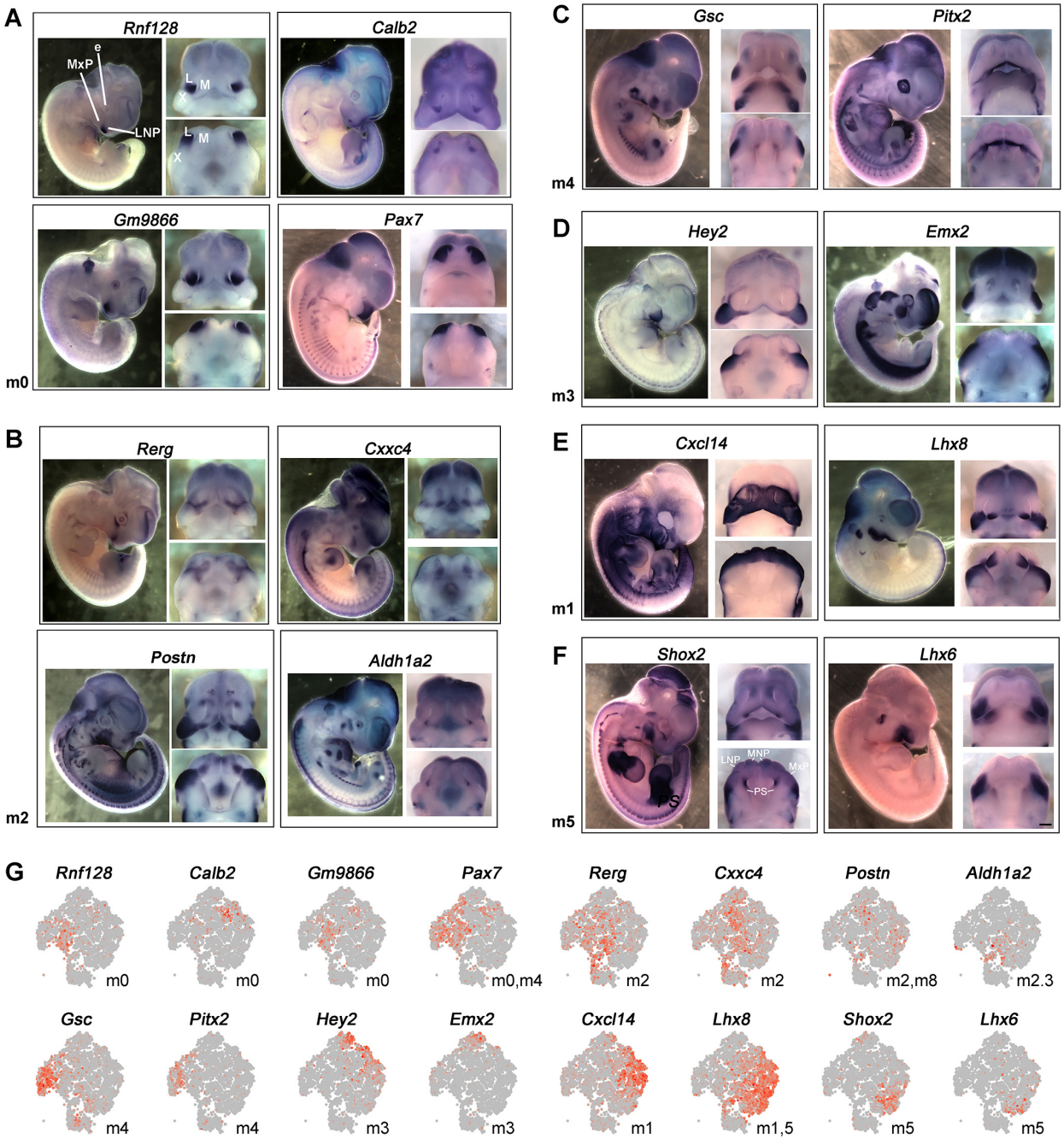

Figure S5. Whole mount *in situ* hybridization of cluster specific mesenchymal markers on embryos reveals localization to particular anatomical domains.

(**A-F**) The panels are arranged according to probes shown in italics and cluster shown at the bottom left. For each gene, three panels are shown. The left panel shows the lateral view of the whole embryo, the top right panel shows the frontal view of the head and the bottom right panel shows the palatal view of the roof of the mouth. Note that the majority of the frontal views also have the mandibles removed, with the exception of *Pax7*, *Gsc*, *Pitx2*, *Shox2*, and *Lhx6.* Most embryos are at E11.5, but there is some slight variation between E11-12 timepoints. (**A**) Expression patterns of m0 marker genes, *Rnf128*, *Calb2*, and *Gm9866* localize to the

anterior/distal LNP. *Pax7* is a broader LNP marker and is representative of both clusters m0 and m4. (**B**) Expression patterns of m2 marker genes, *Rerg*, *Cxxc4*, *Postn*, and *Aldh1a2*. All four genes are expressed in the mesenchyme near the ectodermal seams of fusing LNP and MNP (nasal fin), and – with the exception of *Aldh1a2* - also map to the nasolacrimal groove. (**C**) Expression patterns of m4 marker genes, *Gsc* and *Pitx2*. *Gsc* displays modest expression in the more dorsal FNP mesenchyme. *Gsc* is also strongly expressed in lateral regions of the MxP, but this region was not included in our microdissected samples. The expression of *Pitx2* in the FNP mesenchyme was not detected by whole mount *in situ* hybridization. However, it is clear that *Pitx2* is expressed in the posterior and medial part of LNP by *in situ* hybridization on sections shown in Fig S6C. This discrepancy could be caused by the insufficient penetration of the probes into deep tissues in whole mount *in situ* hybridization. *Pitx2* also shows strong expression in the roof of the mouth corresponding to the ectoderm of the dental lamina. (**D**) Expression patterns of m3 marker genes, *Hey2* and *Emx2,* are mainly associated with the MxP. (**E**) Expression patterns of m1 marker genes, *Cxcl14* and *Lhx8,* associated with the anterior and medial MxP mesenchyme. Note that *Cxcl14* is strongly expressed in the surface ectoderm, preventing assessment of its mesenchymal expression in whole mount. Mesenchymal expression can be visualized on sectioned material (see Figure 3E). *Lhx8* exhibits strong expression in the MxP, weaker expression in the LNP, and is also expressed in the MNP. (**F**) Expression patterns of m5 marker genes, *Shox2* and *Lhx6*. Although *Lhx6* is expressed in more lateral regions of the MxP, this region was absent from our microdissections. Instead, for this m5 cluster, we are detecting the expression of these two genes in the nascent MxP derived palatal shelves. (**G**) Feature plots for the marker genes used for whole mount *in situ* hybridization in A-F with gene names on top and clusters at bottom right for each gene. *Postn* is a marker gene for both m2 and m8. *Lhx8* is a marker gene for both m1 and m5. e, eye; LNP or L, lateral nasal process; MNP or M, medial nasal process; MxP or X, maxillary prominence; PS, palatal shelf. Scale bar, 500μM.

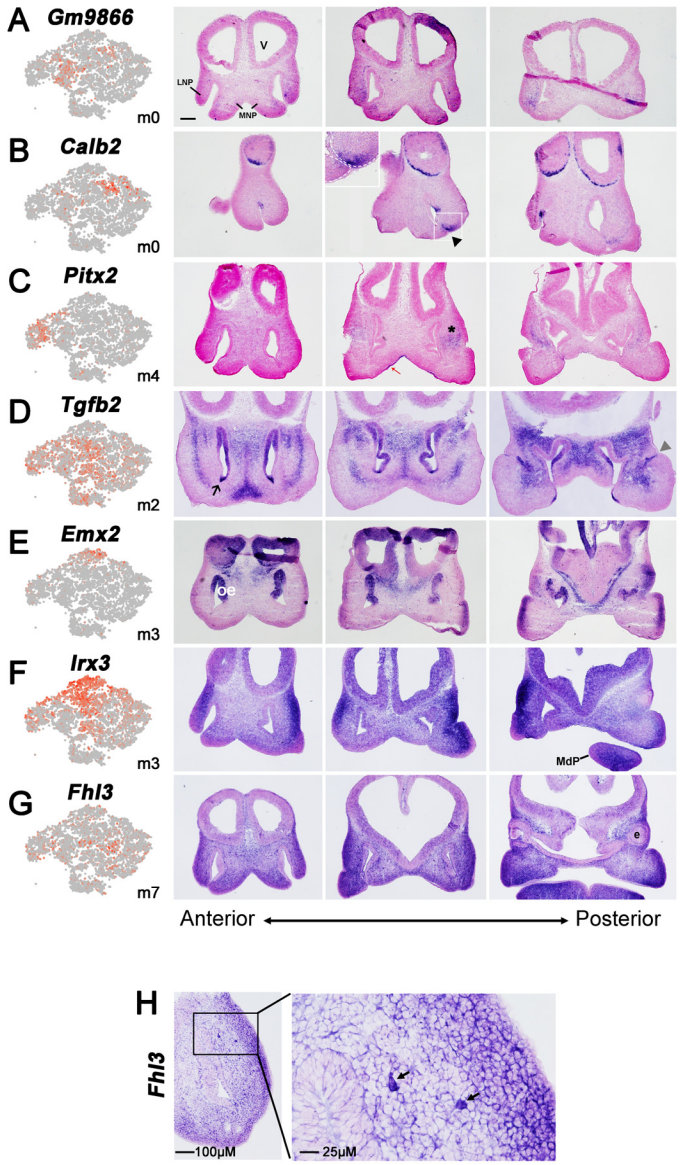

Figure S6. RNA *in situ* hybridization for mesenchymal markers on E11.5 facial sections.

(**A-G**) Feature plots (left panel) and *in situ* hybridization on frontal sections (three right panels, anterior to posterior as indicated by double headed arrow beneath panels) of E11.5 mouse face for mesenchymal marker genes *Gm9866* (A), *Calb2* (B), *Pitx2* (C), *Tgfb2* (D), *Emx2* (E), *Irx3* (F) and *Fhl3* (G) for clusters m0, m0, m4, m2, m3, m3, and m7, respectively. Arrowhead in B indicates the expression of *Calb2* at the anterior tip of the LNP. Inset in B shows more detailed image of the area of fusing lambdoid junction indicated by white rectangle. White dashed lines represent the boundary between ectodermal and mesenchymal layers. Asterisk in C indicates the expression of *Pitx2* in the mesenchyme of lateral nasal process, while red arrow indicates the ectodermal expression of *Pitx2* within the oral cavity. In D, besides marking m2, *Tgfb2* is detected in the ectoderm between the LNP and MNP (arrow) and in the NLG (grey arrowhead) in D. Scale bar, 200μM. (**H**) Expression of *Fhl3* at higher magnification. Arrows indicate the cells

with higher expression of *Fhl3* are potentially dividing based on the cell shape. Sections are counterstained with nuclear fast red. e, eye; LNP, lateral nasal process; MdP, mandibular prominence; MNP, medial nasal process; MxP, maxillary prominence; oe, olfactory epithelium; V, ventricle.

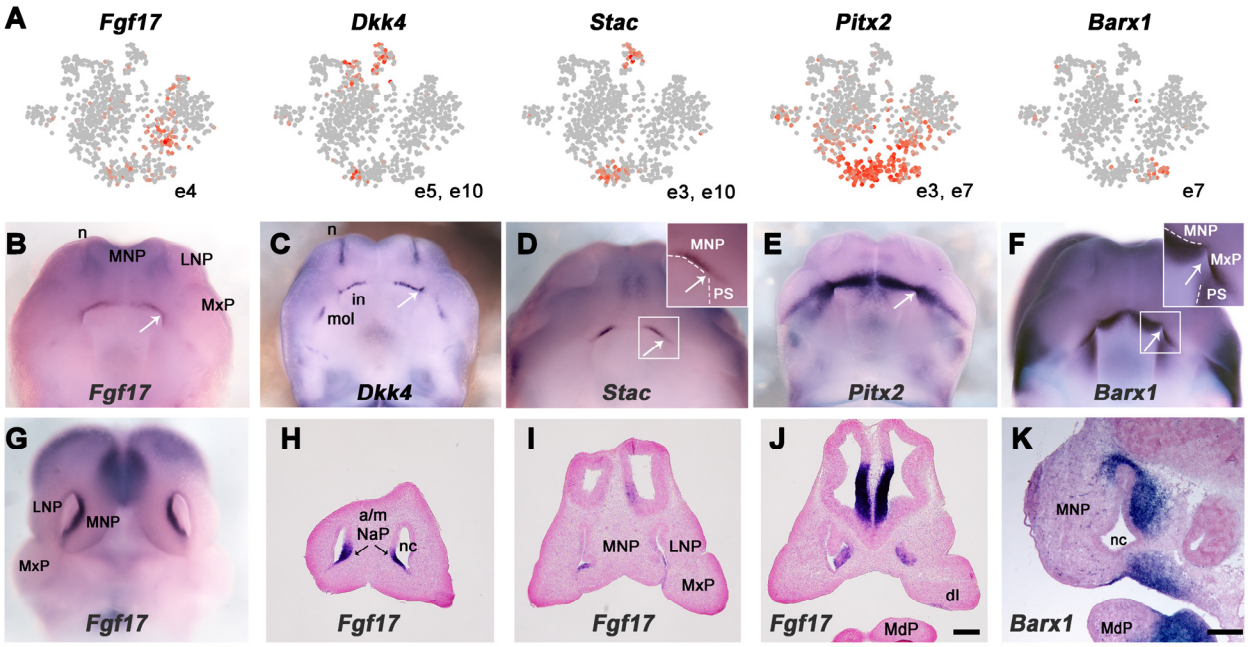

Figure S7. Anatomical mapping of ectoderm clusters to the epithelia of the oral and nasal cavities.

(**A**) Feature plots for *Fgf17, Dkk4*, *Stac*, *Pitx2*, and *Barx1*, with the associated cluster shown at the bottom right. (**B-G**) Palatal (B-F) or frontal (G) views of whole mount RNA *in situ* hybridization for *Fgf17* (B, G), *Dkk4* (C), *Stac* (D) *Pitx2* (E), and *Barx1* (F) between E11-E12. The mandible has been removed to visualize the oral epithelia associated with the roof of the mouth. White arrows indicate the choanal pits as landmarks in B-F. Insets in D and F show more detailed images of the areas indicated by the white rectangles with white dashed lines showing the boundaries of MNP and PS. (**H-J**) *In situ* hybridization of *Fgf17* on E11.5 frontal sections from anterior to posterior. (**K**) *In situ* hybridization of *Barx1* on E11.5 sagittal section. The oral epithelial cluster e3 marker *Stac* is expressed in the anterior part of the oral cavity (D). Similar staining domains are also apparent for *Fgf17* and *Dkk4,* consistent with their presence in e3 on the feature plot even though these genes are not called as specific e3 markers bioinformatically (Table S5). In contrast, *Pitx2* is expressed in both the anterior e3 and posterior e7 domains. Although *Barx1* is an e7 marker, the specific domain of *Barx1* expression in the ectoderm is difficult to determine by whole mount analysis (F) as this gene is more highly expressed in the underlying mesenchyme of the roof of the mouth. Ectodermal *Barx1* expression is apparent in (K) along with a more posterior mesenchymal expression domain. In the nasal cavity *Fgf17* also marks cluster e4, positioned on the anterio-medial side of the nasal pit (a/m NaP). Expression is also strongly detected in the ventral half of the medial walls of the diencephalic ventricles. Sections are counterstained with nuclear fast red. dl, dental lamina; in, incisor; LNP, lateral nasal process; MNP, medial nasal process; MdP, mandibular prominence; mol, molar; MxP, maxillary prominence; n or nc, nasal cavity; PS, palatal shelf. Scale bars for A-G, 500μm; H-J and K, 200μm.

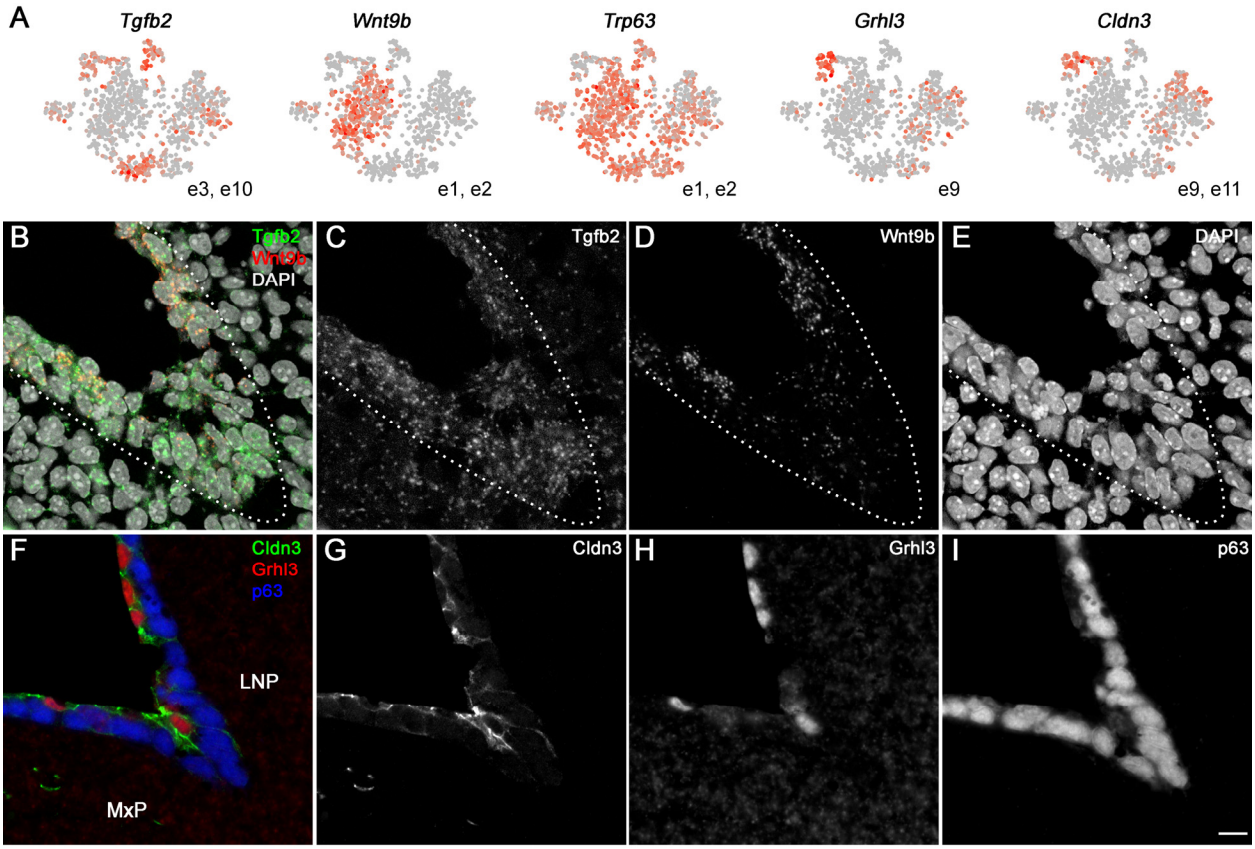

Figure S8. Unique behavior of basal cells in the fusion zone of the nasolacrimal groove.

(**A**) Feature plots for *Tgfb2, Wnt9b*, *Trp63*, *Grhl3*, and *Cldn3* with the associated cluster shown at the bottom right. (**B-E**) RNAscope fluorescence *in situ* hybridization shows reduced *Wnt9b* expression (red) at the base of the nasolacrimal groove near the fusion point, where a disorganized mass of cells express *Tgfb2* (green). Nuclei are stained with DAPI and the dashed line outlines the epithelia. (**F-I**) Immunofluorescent images of p63 (blue), Grhl3 (red) and Cldn3 (green) at the groove between the LNP and the MxP, showing organized bilayer of basal cells and flattened periderm away from the groove and disorganized periderm at the fusion point. Scale bar 10μm.

Table S1. Marker genes for the five clusters from the C57LJ dataset. 'avg_logFC' is log2 of the ratio of mean expression for all cells in cluster vs all other cells. 'pct.1' and 'pct.2' are percent of cells in or outside the cluster with detectable expression of the gene. 'p_val' and 'p_val_adj' show the probability that a gene marks the cluster. 'pct.ratio', the ratio of pct.1 and pct.2, and 'pct. diff', the difference between pct.1 and pct.2, are additional measures of specificity. The table has been sorted according to cluster and 'avg_logFC'.

Click here to Download Table S1

Table S2. Marker genes for mesenchymal clusters from CrectLJ dataset. Columns are as for Table S1. The table has been sorted according to cluster and 'p_val'.

Click here to Download Table S2

Table S3. Spatial assignment of the mesenchymal clusters in relation to the E11.5 mouse upper face and microdissected region. The left column shows the main cluster identifier, showing the color code from Figure 2. The m0* subcluster, which is defined by the expression of *Calb2,* and is confined to the most anterior/distal tip of LNP, is further illustrated by the dotted patterning. For m2, the m2.0 cluster that associates with NLG is further illustrated by dotted patterning. The m2.3 cluster is not shown for simplicity, but maps at the lambdoid junction. For each cluster, we also show assigned anatomical positions and pertinent markers. The schematic views and labels are as for Fig S1. The approximate domains of expression for each cluster are shown by color coding on these cartoons. If no color is shown on a particular cartoon, it is because no representatives of the cluster can be observed in that view or section.

Note that our assignment and bioinformatics analysis of clusters is based solely upon the limited cell population within the three-dimensional tissue space defined by microdissection even though we show some patterns extending beyond this region in accordance with in situ hybridization data.

Cluster	Position	Marker Genes	Frontal	Lateral	Ventral	Anterior Section	Posterior Section
m0 m0*	Anterior and medial LNP	*Rnf128* *Calb2,* *Gm9866*	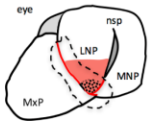	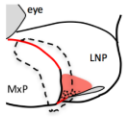	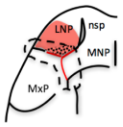	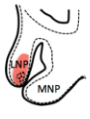	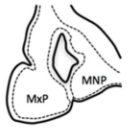
1	Anterior and medial MxP	*Cxcl14* *Lhx8* *Dlx5*	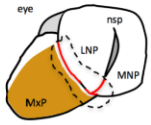	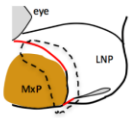	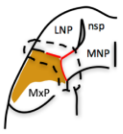	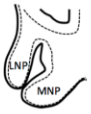	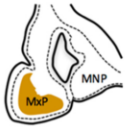
m2 m2.0	Cells adjacent to fusing ectoderm	*Cxxc4* *Rerg* *Tgfb2*	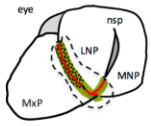	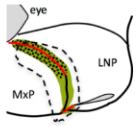	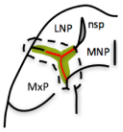	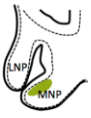	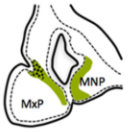
m3	Cells adjacent to surface ectoderm	*Hey2* *Emx2* *Irx3*	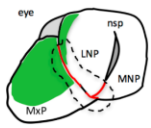	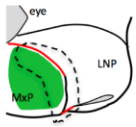	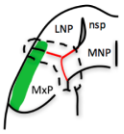	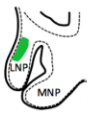	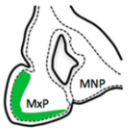
m4	Posterior and medial LNP	*Gsc* *Pitx2* *Osr1*	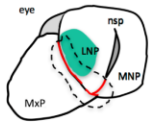	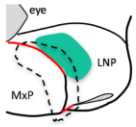	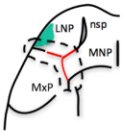	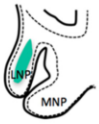	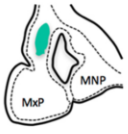
m5	Palatal shelf	*Shox2* *Lhx6* *Asb4*	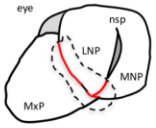	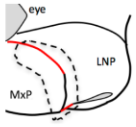	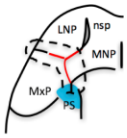	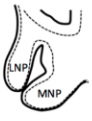	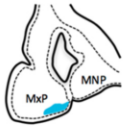
m6	Chondro-progenitors	*Col9a1* *Sox9* *Flrt2*	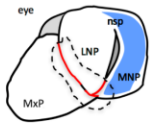	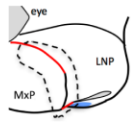		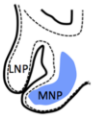	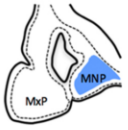
m7	"Ambiguous"	*Fhl3* *Notch2* *Rbm15*	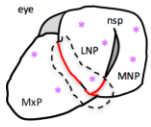	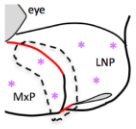	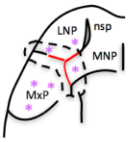	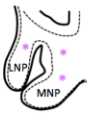	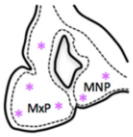
m8	Schwann cell progenitors	*Sox10* *Foxd3* *Fabp7*					

Table S4. Marker genes in the five m2 subclusters, m2.0-2.4. Columns are as for Table S1. The table has been sorted according to cluster and 'p_val'.

Click here to Download Table S4

Table S5. Marker genes for ectodermal clusters from C57LJ dataset. Columns are as for Table S1. The table has been sorted according to cluster and 'p_val'.

Click here to Download Table S5

Table S6. Spatial assignment of the ectodermal clusters in relation to the E11.5 mouse upper face and microdissected region. The left column shows the main cluster identifier, showing the color code from Figure 5. The e0/e11, e1/2 and e5/10 clusters are shown together as, with the exception of e5 which maps to the NLG, we did not distinguish between these clusters anatomically. Cluster e8 has been omitted since we suspect that these are a mixed population of cell doublets. We also show assigned anatomical positions and pertinent markers. The schematic views and labels are as for Fig S1. The approximate domains of expression for each cluster are shown by color coding on these cartoons. If no color is shown on a particular cartoon, it is because no representatives of the cluster can be observed in that view or section. Note that our assignment and bioinformatics analysis of clusters is based solely upon the limited cell population within the three-dimensional tissue space defined by microdissection even

though we show some patterns extending beyond this region in accordance with in situ hybridization data.

Cluster	Position	Marker Genes	Frontal	Lateral	Ventral	Anterior Section	Posterior Section
e0/e11	Olfactory epithelium	*Rprm* *Pcdh19* *Ctxn3* *Ebf1* *Mgp* *Lhfp*	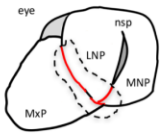	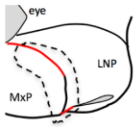	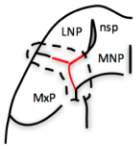	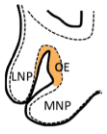	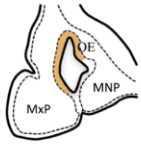
e1/2	Surface ectoderm	*Wnt9b* *Wnt3* *Lmo1* *Robo2* *Pcp4l1*	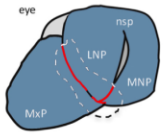	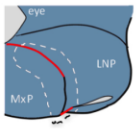	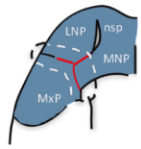	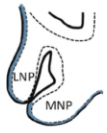	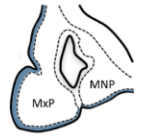
e3	Dental	*Shh* *Fgf8* *Lmo2*	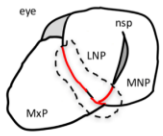	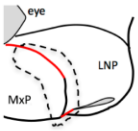	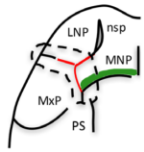	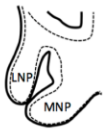	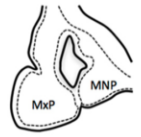
e4	Anterior medial olfactory epithelium	*Fgf17* *Mecom* *Clu*	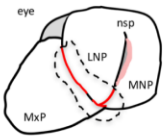	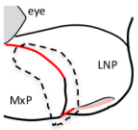	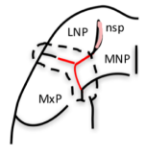	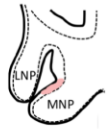	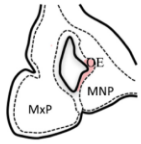
e5/e10	Nasal lacrimal groove and fusion zone	*Adamts9* *Barx2* *Dkk4* *Stac*	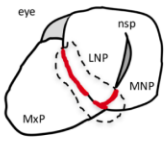	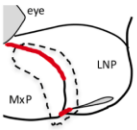	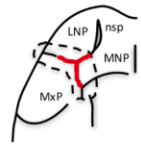	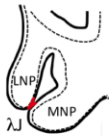	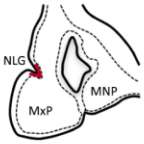
e6	"Ambiguous"	*Slc39a1* *Spry2* *Slc25a5*	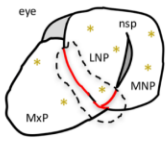	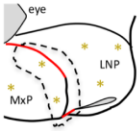	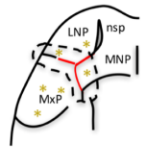	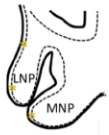	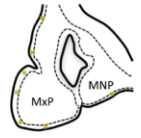
e7	Palate	*Barx1,* *Gm12446* *Dmrt2*	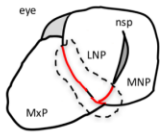	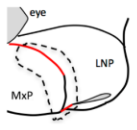	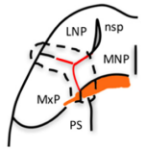	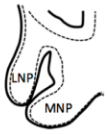	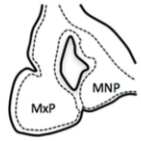
e9	Periderm	*Gabrp* *Rhov* *Lypd3*	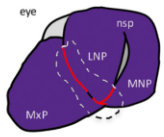	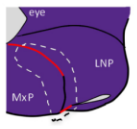	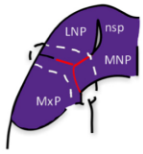	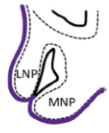	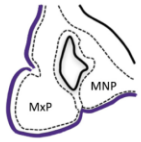

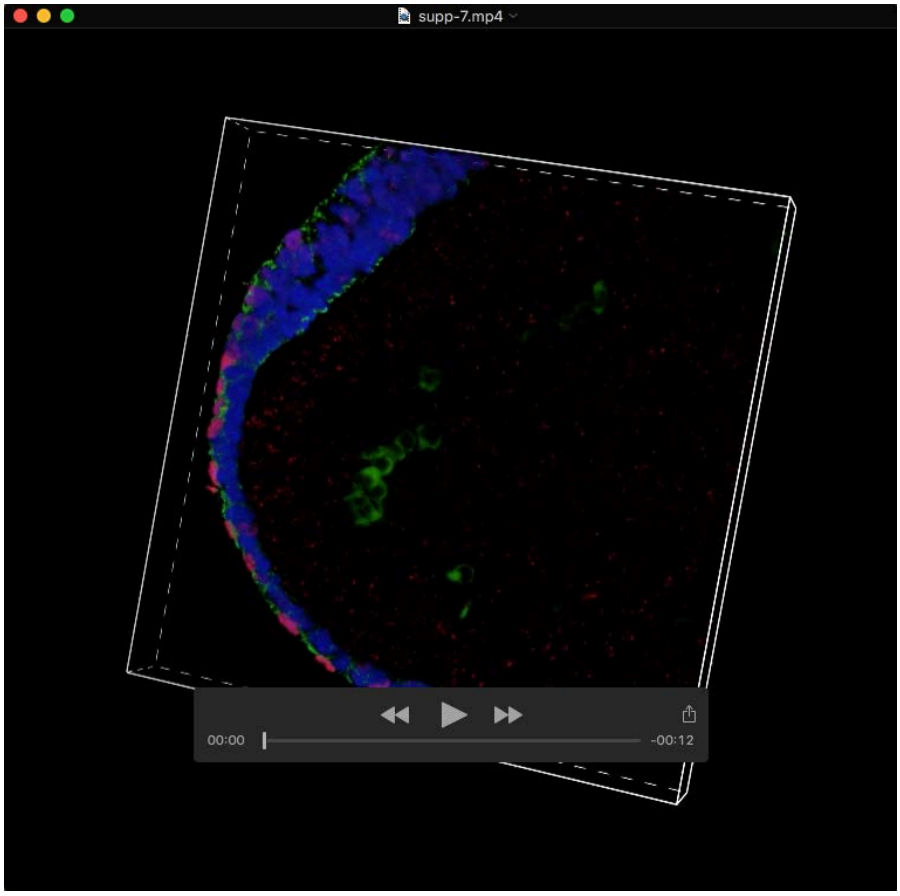

Movie 1. Volume reconstruction of a 14μm section from MNP shows nuclear morphologies. A volumetric protection of a confocal Z-stack, whose mid-stack optical section was shown in Figure 8B. It shows MNP at the border between the surface epithelium and olfactory pit epithelium at E11.0, 4 sections anterior to the fusion site and about 12 sections from the tip of the nasal process. Grhl3 (red) marks periderm nuclei; p63 (blue) marks basal cell nuclei and also weakly marks some periderm nuclei; Cldn3 (green) marks epithelial junctions of periderm and olfactory pit cells. The nuclei designated Figure 8B1 and 8B2 as round, intermediate and flat are included. Rotations of volume projections demonstrate that these represent true nuclear morphologies and are not an artifact of viewing angle or plane of section.